

High-resolution radio observations of Markarian 3

M. J. Kukula,¹ T. Ghosh,² A. Pedlar,¹ R. T. Schilizzi,³ G. K. Miley,⁴ A. G. de Bruyn³ and D. J. Saikia⁵

¹Nuffield Radio Astronomy Laboratories, Jodrell Bank, Macclesfield, Cheshire SK11 9DL

²Arecibo Observatory, PO Box 995, Arecibo, Puerto Rico 00613, USA

³Netherlands Foundation for Research in Astronomy, Postbus 2, AA, Dwingeloo NL-7990, The Netherlands

⁴Sterrewacht Lieden, PO Box 9513, RA, Leiden NL-2300, The Netherlands

⁵GMRT Project, Tata Institute of Fundamental Research, Poona University Campus, Ganeshkhind, Pune 411007, India

Accepted 1993 April 28. Received 1993 April 5; in original form 1993 January 22

ABSTRACT

We present high-sensitivity 5-GHz MERLIN and 15-GHz VLA observations of the Seyfert nucleus of Markarian 3, with angular resolutions of 40 and 250 mas respectively. Our 5-GHz MERLIN map reveals the best example to date of a pair of highly collimated radio jets in a Seyfert nucleus. The jet system is 2 arcsec (~ 600 pc) in extent and less than 50 mas across, and lies along P.A. 84° . Embedded in the jets are a number of compact components, and the western side terminates in a bright lobe containing a hotspot. The component at RA (1950) $06^{\text{h}} 09^{\text{m}} 48^{\text{s}}.423$, Dec. (1950) $71^\circ 03' 10''.42$ is unresolved and is the closest to the peak of the optical continuum emission. We therefore identify this as the radio core. Overall the source has a steep spectrum ($\alpha \sim 1$, where $S \propto \nu^{-\alpha}$). The jet shows a slight 'S'-shaped curvature, and this is also seen in images of the optical narrow-line emission. We discuss these observations in relation to starburst models for Seyfert activity, which we feel are difficult to reconcile with the structure of Mrk 3, the high degree of collimation being more consistent with the idea of a compact 'central engine'.

Key words: galaxies: individual: Mrk 3 – galaxies: jets – galaxies: Seyfert – galaxies: starburst – radio continuum: galaxies.

1 INTRODUCTION

The detailed radio and optical emission-line properties of Seyfert nuclei, and their mutual correlations, provide important clues to the underlying processes occurring in active galactic nuclei (AGN). With the *Hubble Space Telescope* (*HST*), optical resolutions of 50 mas can now be achieved, and radio images of a similar quality are required if useful comparisons are to be made. Markarian 3 (Mrk 3) was one of several Seyfert galaxies to be observed by the upgraded MERLIN at 5 GHz (6 cm) with a resolution of ~ 40 mas. Observations were also made at 2 cm with the VLA in A-configuration and a resolution of 250 mas.

Mrk 3 is a type 2 Seyfert galaxy situated at a distance of 55 Mpc (assuming $H_0 = 75 \text{ km s}^{-1} \text{ Mpc}^{-1}$) so that 1 arcsec ~ 270 pc (Khachikian & Weedman 1974). There has been some debate over the Hubble type of the host galaxy; Adams (1977) classified it as SB0, but subsequent studies by Jenkins (1981) and Wagner (1987) imply that the host is in fact an elliptical galaxy with a small, edge-on disc of gas and stars which rotates differentially. This is unusual, since Seyfert nuclei normally occur in spiral galaxies whilst

elliptical systems tend to be the hosts of the larger and more powerful radio galaxies. In fact, the radio power of Mrk 3 is only an order of magnitude less than that of the weaker radio galaxies such as 3C 305, but its emission-line ratios, and the fact that the radio structure lies entirely within the nucleus of the host, place Mrk 3 firmly in the category of Seyferts.

Pedlar, Unger & Booler (1984) measured the H I mass of the galaxy and found a lower limit of $7 \times 10^9 M_\odot$, comparable to that of typical S0 and spiral galaxies, and an order of magnitude higher than that of elliptical galaxies. An abnormally large H I mass could be the result of an interaction with the nearby spiral galaxy UGC 3422, but Wagner finds no sign of disruption in the optical isophotes of Mrk 3, implying that only the extreme outer regions of the galaxy can be affected.

Emission lines have been detected from a region 11×13 arcsec² in extent in P.A. 113° (Weedman 1973; Wilson et al. 1980), but O [III] and H α (1-arcsec resolution) maps of the narrow-line region (NLR) by Haniff, Ward & Wilson (1988) show a 4-arcsec, elongated structure in P.A. 82° , with the fainter isophotes twisting to higher P.A.s further from the nucleus. A more extended emission-line region, 12×3

arcsec² in extent, lies in the differentially rotating gaseous disc along P.A. 112° (Wagner 1987).

Early radio observations by Wilson et al. (1980) at 6 and 2 cm revealed a double source 1.5 arcsec across, straddling the optical nucleus in P.A. \sim 80°. Pedlar et al. (1984), working at 73 and 18 cm, found a linear feature 2.5 arcsec (\sim 600 pc) long in P.A. 84° enclosing three steep-spectrum components. This was interpreted as evidence for collimated ejection, with the brighter, western component as the core and a jet with two elongated knots extending to the east.

Mrk 3 was one of several Seyfert galaxies to be observed by the upgraded MERLIN at 5 GHz (6 cm). The present MERLIN observations represent an improvement in resolution by a factor of 5, and in sensitivity by an order of magnitude, over previous radio work.

2 THE OBSERVATIONS

Mrk 3 was observed for 13.5 h in 1992 January, using MERLIN (Davies, Anderson & Morison 1980) at a wavelength of 6 cm (4.997 GHz). The inclusion of the new 32-m antenna at Cambridge gives the array a maximum baseline length of 217 km (3.6 M λ at 5 GHz). Left-hand circular polarization with a 7-MHz bandwidth was used, since MERLIN's dual-polarization, wide-band mode was still being developed at the time of the observations.

The point source 0552 + 398 (DA 193) was used to determine the flux density calibration; by comparison with 3C 286 (Baars et al. 1977), its flux density was found to be 6.6 Jy at 5 GHz. In order to obtain high positional accuracy in our images, phase-referencing was used, with 0604 + 728 as the phase calibrator. Self-calibration solutions for 0604 + 728 were used to estimate the antenna gain and phase corrections for Mrk 3.

The initial amplitude calibration and editing were performed within the MERLIN-specific OLAF package, and the files were then transferred to AIPS where they were phase-calibrated. Once the calibration was complete, the data were Fourier-transformed and CLEANED with restoring beams of 65 and 40 mas (FWHM) for natural and uniform weighting respectively. After self-calibration and individual reweighting of the MERLIN antennas, the sensitivities achieved were 140 μ Jy beam⁻¹ for natural weighting and 220 μ Jy beam⁻¹ for uniform weighting, with a dynamic range of 500:1.

A-configuration observations of Mrk 3 were made with the VLA in 1987 September at a wavelength of 2 cm (14.9 GHz). The total integration time was 3 h, but the southwest arm of the VLA was not available during the observations, and the *uv*-coverage achieved was therefore less than optimal. After self-calibration and deconvolution, the uniformly weighted image was restored with a 250-mas beam and a sensitivity of 150 μ Jy beam⁻¹. With natural weighting the sensitivity achieved was 100 μ Jy beam⁻¹ and the resolution 300 mas.

3 RESULTS

Fig. 1 shows the 2-cm, uniformly weighted VLA map, and in Figs 2(a) and (b) we present the uniformly and naturally weighted, 6-cm MERLIN maps respectively. The radio structure at 2 cm is consistent with the findings of Pedlar et al. and Wilson et al., consisting of two components in P.A.

84° linked by a 'jet'. The total flux density at this frequency is 75 mJy. By comparing the flux densities at 6 and 2 cm, spectral indices were calculated for the 'jet' and the two components (Table 1); we find that the entire source has a steep spectrum ($\alpha \sim 1$, where $S \propto \nu^{-\alpha}$), consistent with the values obtained by Pedlar et al. between 73 and 18 cm.

A more complex structure is revealed in the 6-cm MERLIN image. Eight distinct components are visible (labelled 1 to 8 in Fig. 2b) within a highly elongated structure having a total flux density of 0.29 Jy.

The bright western component (component 8) is resolved, and is clearly an extended object. A slice through the major axis of this component (Fig. 3) reveals a double-peaked internal structure. Meanwhile, the eastern feature of the 2-cm map appears at 6 cm as a triple source (components 2, 3 and 4) lying along P.A. 82°. There is also some faint emission \sim 0.1 arcsec further east, which curves to P.A. \sim 110° and corresponds to that detected at 2 cm. A string of elongated blobs links the eastern and western components, and together they form the 'jet' seen in the 2-cm map. Apart from component 8, all of the radio knots are unresolved in the direction perpendicular to the axis of the 'jet', even in the uniformly weighted image with its 35-mas restoring beam (Fig. 2a).

When natural weighting is applied to the data (Fig. 2b), we find evidence for continuous low-level emission along the entire length of the 'jet'. The position angle of the structure increases from $80 \pm 5^\circ$ at the middle to $\sim 95^\circ$ towards the extremities, giving the object an 'S'-shaped appearance.

The flux densities of the components were determined by fitting a two-dimensional Gaussian function to each object. Assuming that the components are ellipsoidal in shape with a filling factor of 1, we have estimated the energy density, magnetic field strength and pressure for each object using equipartition arguments (Moffet 1975). Such calculations are notoriously unreliable and, since all but component 8 are unresolved in the direction perpendicular to the 'jet', we obtain only lower limits for these parameters. We present the results in Table 1.

Due to the lack of high-resolution images at other frequencies, we were unable to calculate spectral indices for the individual components. Estimates were obtained by convolving the 5-GHz map with a 250-mas Gaussian beam, and comparing the resulting surface brightnesses with those of the 15-GHz map. Since several of the components are merged together at this resolution, only average spectral indices were found.

The main unknown in the standard equipartition argument is the ratio of the energy in relativistic protons to that in relativistic electrons. We have assumed a value of 1; with the other frequently used value of 100 the magnetic field is increased by a factor of ~ 3 , and the pressure and energy densities by a factor of 10. Our values are in reasonable agreement with those of Pedlar et al. (1984).

4 DISCUSSION

Both our 6- and 2-cm results show a linear structure, and are consistent with the idea of collimated ejection of material along P.A. \sim 80°. We interpret this structure as a double-sided radio jet emerging from a compact core, which we identify with component 4 [RA (1950)

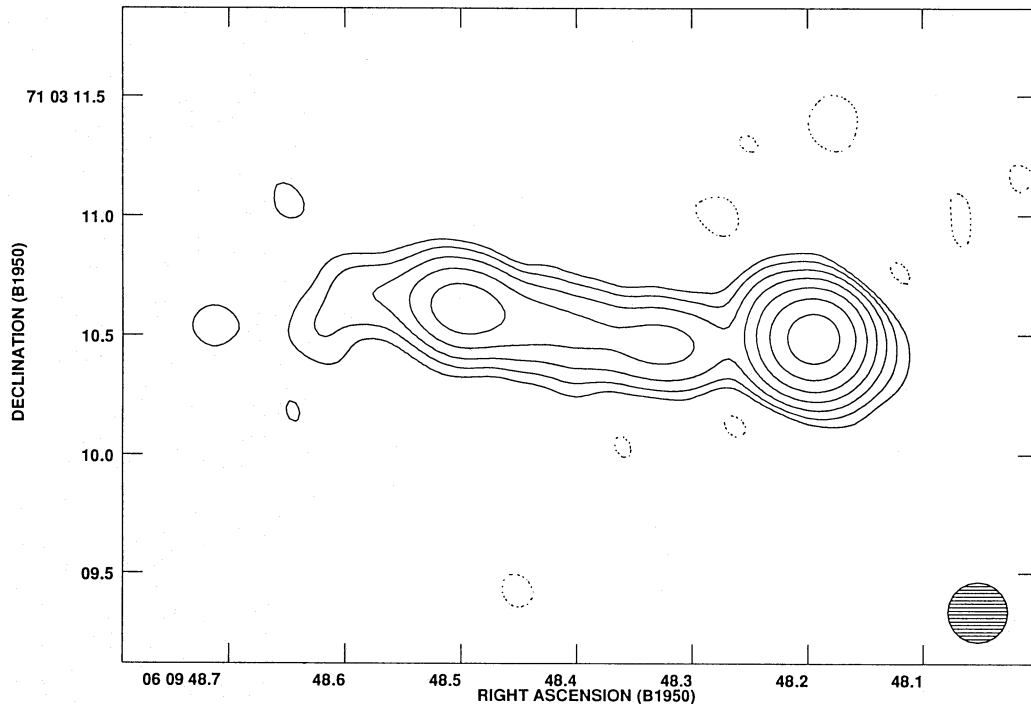


Figure 1. Contour map of the uniformly weighted 14.9-GHz image made with the VLA in A-configuration. The restoring beam (shaded circle) has a FWHM of 250 mas. The sensitivity is $150 \mu\text{Jy beam}^{-1}$. Contour levels are at $-450, 450, 900, 1800, 3600, 7200, 14400$ and $28800 \mu\text{Jy}$. The peak flux is 43 mJy beam^{-1} .

$06^{\text{h}} 09^{\text{m}} 48^{\text{s}}.423 \pm 0.006$, Dec. (1950) $71^{\circ} 03' 10''.42 \pm 0.01$]. This component is unresolved, even with the 35-mas restoring beam of the uniformly weighted 5-GHz map, and is situated within the 0.25-arcsec uncertainty in the position of the optical nucleus [RA (1950) $06^{\text{h}} 09^{\text{m}} 48^{\text{s}}.42$, Dec. (1950) $71^{\circ} 03' 10''.7$] as determined by Clements (1981). In order to confirm the identification of the core component, high-resolution images at several frequencies are required. Evidence of variability, a flatter spectrum and little or no polarization would all strengthen the case for this component being the core; it should also be unresolved in VLBI measurements.

In this scheme, the bright component 8 becomes a radio lobe at the terminus of the western jet, and there is substructure which is reminiscent of the 'hotspots' observed in more powerful AGN. There does not appear to be a corresponding object at the terminus of the eastern jet, which ends ~ 0.5 arcsec (140 pc) from the nucleus. The other radio components could be analogous to the knots seen in the jets of radio galaxies.

4.1 The radio jets in Markarian 3

In many Seyfert nuclei there is strong evidence for the collimated ejection of radio plasma in the form of discrete blobs or plasmons, but the evidence for continuous jets is less convincing. Observations often show radio components which are elongated in the direction of the ejection axis (as in our 15-GHz VLA image of Mrk 3), but this in itself does not constitute proof of a jet. Indeed, some models of the collimation mechanism in less energetic AGN favour a situation in which the stream of material is periodically 'pinched off' to produce a series of plasmons (Smith et al. 1983).

Bridle & Perley (1984) define a 'jet' as a structure that is at least four times longer than it is wide and that is clearly separable from any extended structure, either spatially or by brightness contrast. The structure seen in Mrk 3 satisfies these conditions almost as well as the radio jet in Virgo A, and more convincingly than many undisputed jets in other AGN. Apart from component 8, the entire structure is unresolved in the transverse direction so that the length-to-width ratio is $\geq 25:1$. We fail to detect any emission outside the jet, although it is possible that the lack of very short baselines in MERLIN could cause us to miss some extended emission. To our knowledge, Mrk 3 is the first Seyfert galaxy to show such clear evidence for a radio jet, and this may have important consequences for models of the ejection mechanism as well as the way in which Seyferts are considered in terms of the so-called 'Unified Schemes' for AGN.

4.2 Consequences for models of Seyfert nuclei

The energy densities and magnetic fields of the individual radio components (listed in Table 1) are several orders of magnitude higher than those of typical supernova remnants. They are also at least an order of magnitude more luminous than the radio supernovae of Weiler, Sramek & Panagia (1986). This, together with the linear disposition of the knots along P.A. $\sim 80^{\circ}$ and their elongation in the same direction, seems to rule out the possibility of their being the result of individual supernovae.

However, Terlevich & Melnick (1987) suggest that the radio emission of Seyfert galaxies could be the result of supernova activity in a dense nuclear star cluster or starburst region, rather than ejection along the axis of an accretion

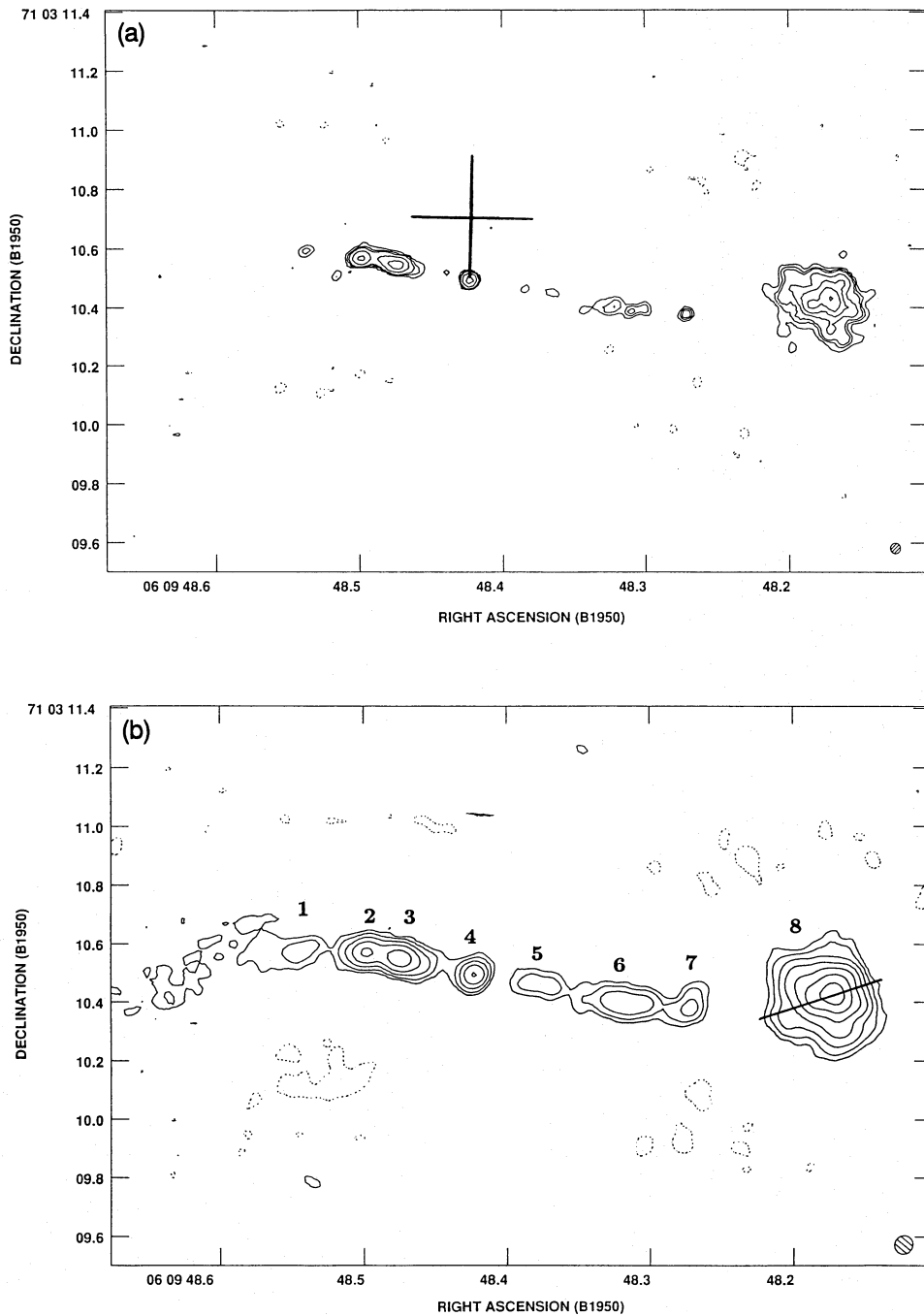


Figure 2. (a) Contour map of the uniformly weighted 5-GHz MERLIN image. The resolution is 35 mas and the sensitivity $220 \mu\text{Jy beam}^{-1}$. The contour levels are $-660, 660, 990, 1320$ and $1650 \mu\text{Jy}$, with subsequent contour intervals increasing by factors of 2. The cross marks the position of the optical nucleus (Clements 1981). (b) The 5-GHz MERLIN image with natural weighting. The resolution is now 65 mas and the sensitivity $140 \mu\text{Jy beam}^{-1}$. Contour levels begin at $480 \mu\text{Jy beam}^{-1}$ and increase by factors of 2. The individual radio components are numbered 1 to 8. The most compact component is number 4, which we believe to be the core. Further low-level emission is now visible along the jet.

disc. They describe how an ensemble of supernova remnants exploding into such an environment would form an expanding bubble. When the bubble reaches the edge of the gaseous nuclear disc, material from the interior is ejected into the low-density outer regions, forming a 'jet'. We feel that this hypothesis is difficult to reconcile with the extremely high

degree of collimation of the Mrk 3 jets and the symmetry implied by the 'S'-shaped curvature. In view of the similarities between the jets in Mrk 3 and those of radio galaxies, it seems reasonable to suppose that a similar mechanism is involved in both. Another factor to weigh against the supernova hypothesis is the nature of the host galaxy of

Table 1. Properties of the radio knots in the 6-cm MERLIN map (Fig. 2).

Component	6-cm Flux density (mJy)	Spectral index α	Distance from nucleus (arcsec)	Physical parameters		
				B_{me} (10^{-7} T)	U_{me} (10^{-8} $J m^{-3}$)	P_{me} (10^{-9} $N m^{-2}$)
1	4.9	0.92	0.75	0.60	0.8	2.7
2	13.1	1.06	0.50	2.00	2.2	7.3
3	23.9	1.06	0.30	2.00	2.1	7.0
4	8.3	1.06	0.00	2.00	2.8	9.3
5	3.7	0.92	0.38	0.95	0.8	2.8
6	11.6	0.92	0.70	0.86	0.7	2.3
7	3.9	0.92	1.00	1.00	1.3	4.3
8	155.6	1.03	1.20	2.00	2.4	8.0

Component 4 is the most compact, and we believe this to be the core. The distances of the other components from the core are measured along P.A. 84° and are given in arcsec. Spectral indices were calculated by smoothing the 6-cm map to the same resolution as the 2-cm map and comparing the flux densities. Since several of the components are merged together at this resolution, we obtained only average values for the spectral index. The parameters B_{me} , U_{me} and P_{me} are the magnetic field, energy density and pressure respectively derived from minimum energy requirements (Moffet 1975), assuming that the energy in relativistic electrons is equal to that in relativistic protons. By comparison, the thermal pressure of the emission-line gas obtained from line-ratio measurements is $0.24 \times 10^{-9} N m^{-2}$ (Briggs et al. 1980).

Mrk 3. Most starburst galaxies are disc systems, whereas Mrk 3 appears to be elliptical, albeit with a small nuclear disc of gas and stars. We would not expect to find starburst activity in a galaxy like Mrk 3.

The discovery of a jet in Mrk 3 indicates that Seyfert nuclei can indeed harbour structures very similar to those seen in classical radio galaxies, though on a much smaller scale. It may be that many other Seyferts are concealing highly collimated continuous structures in their nuclei and that Seyfert jets are in fact a common phenomenon. If this is the case, such objects could prove very useful tools for the study of jet formation mechanisms, since Seyfert galaxies are on the whole much closer than their more powerful cousins, and we are therefore able to observe events on a much smaller spatial scale.

4.3 Comparison with the narrow-line region

During the last 15 years, considerable structural evidence has emerged that the radio sources in AGN interact vigorously with the ambient gas. Several remarkable examples of morphological associations between radio continuum emission and optical line emission have been found (e.g. Heckman 1988, and references therein).

The frequent alignment of the radio and NLR structures along a common axis argues strongly for related collimation mechanisms for the ionizing nuclear continuum radiation (which produces the optical narrow-line emission) and the ejection of the radio plasma. This is a basic feature of many 'Unified Schemes' for AGN in which the radio jets and the ionizing cones of radiation from the central engine lie along the axis of an accretion disc. In Mrk 3 both the radio jets and the NLR lie in P.A. $\sim 80^\circ$ (Fig. 4).

The radio jet in Mrk 3 has a slight curvature which is roughly symmetrical about the nucleus, giving it an 'S'-shaped appearance. Similar bending is seen in other Seyfert

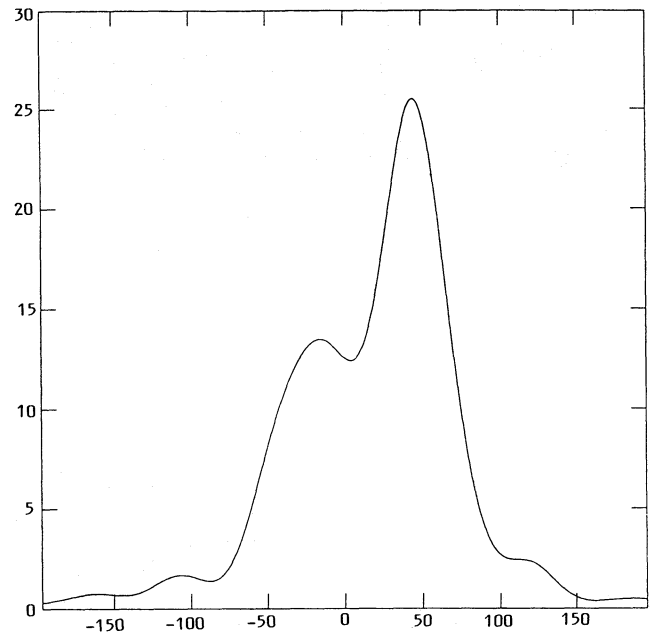


Figure 3. A slice through component 8 of the naturally weighted image (marked in Fig. 2b) showing the double-peaked internal structure. Vertical scale – $mJy beam^{-1}$, horizontal scale – mas.

nuclei, for example in NGC 4151 (Pedlar et al. 1993), as well as in the jets of more powerful radio galaxies. Possible mechanisms include precession of the central engine, ram-pressure bending of the jets by rotating galactic gas, and buoyancy as the relativistic particles of the radio plasma lose energy and drift out of the plane of the gaseous disc. Before these possibilities can be investigated further, H I studies will be required in order to determine the distribution and dynamics of the galactic gas.

A similar curvature in the narrow-line region of Mrk 3 is reported by Haniff et al. (1988). On the scale of 1 to 3 arcsec, the [O III] and H α emission is extended along P.A. 82° but, as the intensity decreases, the major axis of the isophotes twists towards higher position angles (Fig. 3). Recent *HST* images in [O III] λ 5007 and H α , with resolutions similar to our 6-cm maps, reinforce this picture (Z. Tsvetanov, private communication).

A radio galaxy that bears considerable resemblance to Mrk 3 is 3C 305 (Heckman et al. 1982). Here also there is a convincing morphological association, although on a much larger scale of several kpc, between an emission-line gas region and a radio source, with both components displaying a similar 'S'-shaped symmetry. A model involving a merger between an elliptical and a late-type galaxy has been invoked to explain the structure of this object.

In order to explain the observed associations between the radio and NLR structures of Seyferts, Pedlar, Dyson & Unger (1985) derived a model in which the expansion of a radio plasmon drives a shock into the surrounding medium. The shell of shocked material is ionized by the cones of continuum radiation from the nucleus to form the optical NLR. In a related model by Taylor et al. (1989), it is the forward motion of a jet or plasmon that drives a bowshock into the interstellar medium. Material passing through the shock is compressed and heated, and flows back around the plasmon, cooling to the point at which forbidden lines can be emitted. Both scenarios therefore predict a close association between radio components and regions of enhanced narrow-line emission, although in the Taylor et al. model some displacement is expected to allow for the cooling time of the forbidden-line gas. The kinematics of the NLR gas are then

the result of its interaction with the radio plasma, whilst the emission-line properties are due to photoionization by the nuclear continuum source.

The NLR in Mrk 3 is much larger than the radio structure (Fig. 4); this can be explained if the ionizing radiation from the nucleus penetrates beyond the radio jets into the surrounding medium. The internal pressures of the radio knots are at least an order of magnitude higher than the thermal pressure of the narrow-line gas (Briggs et al. 1980; Table 1). If the radio knots are discrete plasmons, they must be expanding into the NLR and we would expect to find enhanced narrow-line emission associated with them. However, in the [O III] images of Haniff et al., there are no distinct features which can be identified with any of the radio components, and we suggest that the knots may mark the sites of recollimation shocks within a jet which is in overall pressure equilibrium with its surroundings. In this case, we would not expect any detailed correspondence between the radio knots and regions of enhanced narrow-line emission, except at the head of the jet where a bowshock might form. The bright lobe at the western end of the radio jet has a double-peaked internal structure (Fig. 3) and would seem to be the best place in which to look for radio/NLR associations in any future studies.

We cannot, however, rule out the possibility that the knots are entrained gas clouds or ejected plasmons moving along the jet, rather than shocks that are stationary within it. Proper motion measurements would help to distinguish between these possibilities, but we estimate that, for velocities of $\sim 0.1c$, observations over several decades would be required in order to detect any movement of the components.

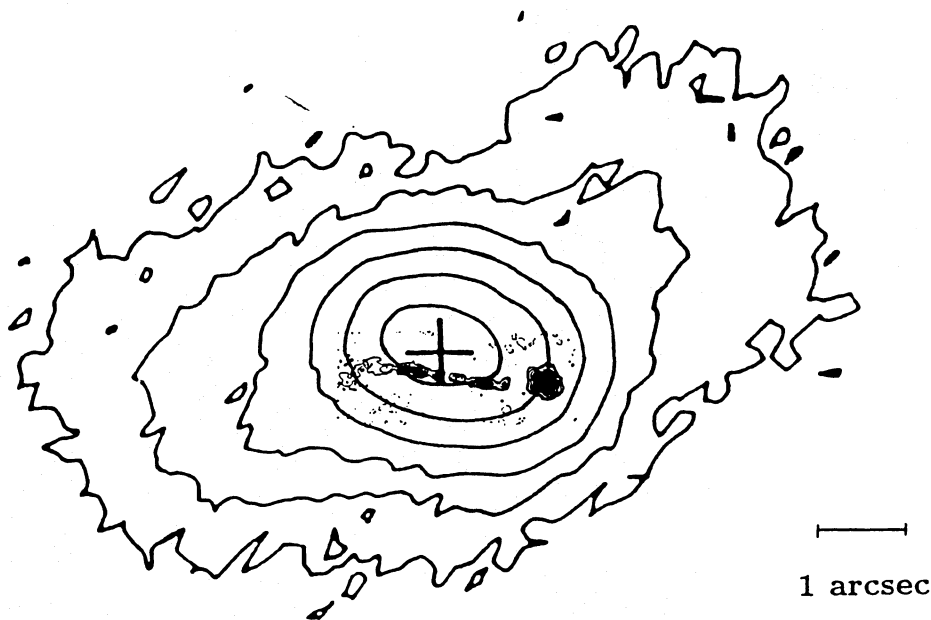


Figure 4. The MERLIN 5-GHz map (grey-scale) superimposed on the [O III] λ 5007 contour map of the NLR of Haniff et al. (1988). We believe that the ~ 0.25 -arcsec uncertainty in the position of the optical peak (marked by the cross) accounts for the apparent offset between the optical and radio cores.

5 CONCLUSIONS

Both the 15- and the 5-GHz measurements are consistent with collimated ejection along P.A. 84°. The structure revealed by the 40-mas resolution of MERLIN is, we believe, the best evidence for a radio jet yet found in a Seyfert nucleus, and if our identification of the radio core is correct, then the jet appears to be double-sided. Embedded in the jet are a number of compact knots, and a large bright radio lobe terminates the western jet. There is a marked similarity between the overall appearances of the radio and optical narrow-line regions, consistent with the hypothesis that the two are closely associated.

The current results highlight the need for further, more comprehensive studies of this object. In order to derive the spectral indices of the individual components, and thus attempt to confirm our identification of the radio nucleus, we require observations at other wavelengths with angular resolutions that are comparable to those of the current work. Also, the wealth of substructure that we observe in the radio-jets, and the association between the radio and forbidden-line emission regions, suggest that Mrk 3 would be an excellent candidate for detailed study of the NLR–radio interaction. Close examination of the structure of the Mrk 3 jets could provide insights into both the ejection mechanism, and the differences and similarities between jets in Seyfert galaxies and those in more powerful AGN.

ACKNOWLEDGMENTS

The National Radio Astronomy Observatory is operated by Associated Universities, Inc., under contract with the National Science Foundation.

REFERENCES

- Adams T. F., 1977, *ApJS*, 33, 19
 Baars J. W. M., Genzel R., Pauliny-Toth I. I. K., Witzel A., 1977, *A&A*, 61, 99
 Bridle A. H., Perley R. A., 1984, *ARA&A*, 22, 319
 Briggs S. A., Boksenberg A., Carswell R. F., Sargent W. L. W., 1980, *MNRAS*, 191, 665
 Clements E. D., 1981, *MNRAS*, 197, 829
 Davies J. G., Anderson B., Morison I., 1980, *Nat*, 288, 64
 Haniff C. A., Ward M. J., Wilson A. S., 1988, *ApJ*, 334, 104
 Heckman T., 1988, in *Proc. IAU Joint Discussion VI, Interaction of Jets with Galaxies*
 Heckman T., Miley G. K., Balick B., van Breugel W. J. M., Butcher H. R., 1982, *ApJ*, 262, 52
 Jenkins C. R., 1981, *MNRAS*, 199, 229
 Khachikian E. Y., Weedman D. W., 1974, *ApJ*, 192, 581
 Moffet A. T., 1975, in Sandage A., Sandage M., Kristian J., *Galaxies and the Universe, Stars and Stellar Systems, Vol. IX*. Univ. Chicago Press, p. 211
 Pedlar A., Unger S. W., Booler R. V., 1984, *MNRAS*, 207, 193
 Pedlar A., Dyson J. E., Unger S. W., 1985, *MNRAS*, 214, 463
 Pedlar A., Kukula M. J., Longley D. P. T., Muxlow T. W. B., Axon D. J., Baum S., O'Dea C., Unger S. W., 1993, *MNRAS*, 263, 471
 Smith M. D., Smarr L., Norman M. L., Wilson J. R., 1983, *ApJ*, 264, 432
 Taylor D., Dyson J. E., Axon D. J., Pedlar A., 1989, *MNRAS*, 240, 487
 Terlevich R., Melnick J., 1987, in Thuan T. X., Montmerle T., Tran Thanh Van J., eds, *Starbursts and Galaxy Evolution*. Edition Frontières, Gif-sur-Yvette, p. 39
 Wagner S. J., 1987, *A&A*, 185, 77
 Weedman D. W., 1973, *ApJ*, 183, 29
 Weiler K. W., Sramek R. A., Panagia N., 1986, *Sci*, 231, 1251
 Wilson A. S., Pooley G. G., Willis A. G., Clements E. D., 1980, *ApJ*, 237, L61